

**RADAR OBSERVATIONS DURING NAME 2004
PART II: PRELIMINARY RESULTS**

Timothy J. Lang*, Rob Cifelli, David Lerach, Lee Nelson, Stephen W. Nesbitt,
Gustavo Pereira, and Steven A. Rutledge
Colorado State University, Fort Collins, Colorado

David Ahijevych and Rit Carbone
National Center for Atmospheric Research, Boulder, Colorado

1. INTRODUCTION

Two-dimensional radar-based regional data products from NAME 2004, detailed in Part I of this study (Lang et al. 2005) - as well as case studies using 3-D volumes from the NCAR S-Pol radar - are being used to understand the climatology of convection in the heart of the North American monsoon in northwestern Mexico and the Gulf of California. In particular, the relative importance of large-scale forcing and the diurnal cycle in organizing and modulating convection is being studied.

Ahijevych et al. (2005) note the typical diurnal behavior of convection along the sea breeze front over the coast, as well as over the complex terrain of the Sierra Madre Occidental (SMO), which peaks in the late afternoon as expected ("undisturbed" regime). In addition, they note very active days ("disturbed" regime) wherein the typical diurnal convection evolves into more organized systems and propagates from the SMO, to the coastal plain where it merges with any existing sea breeze convection, and finally out to sea over the Gulf of California.

In this work, we present preliminary results linking the evolution and structure of precipitation systems to the effects of large-scale forcing and the diurnal cycle. In addition, we will show examples from in-progress case studies of the 3-D microphysical evolution of NAME storms, as well as intercomparisons between S-Pol and a nearby multi-frequency profiler network.

2. DIURNAL CYCLE ANALYSIS

*Corresponding Author Address: Timothy J. Lang, Dept. of Atmospheric Science, Colorado State Univ., Ft. Collins, CO 80523; e-mail: tlang@atmos.colostate.edu

Precipitation features were identified within the Version 1 NAME regional radar composites (0.02° grid spacing) by identifying regions with contiguous pixels (including adjacent corner pixels) of radar reflectivity ≥ 15 dBZ. Nesbitt et al. (2000) used a similar approach identifying precipitation features within the TRMM precipitation radar swath. For this study, features were identified within each time the radar composites were available, and their time of occurrence, location, area, rainfall volume, and number of points greater than 40 dBZ were calculated and stored.

In addition, an ellipse-fitting technique (Nesbitt et al. 2005) is employed on each feature whereby the major and minor axis lengths are calculated from the Eigenvalues of the mass distribution tensor of the raining points within each feature. Twice the major axis of the calculated ellipse is recorded as the feature's maximum dimension (FMD). During the NAME EOP, 199609 features were identified within the composites. Future work will encompass tracking the features in time and space such that storms may be examined in the context of their individual life cycles.

Figure 1 shows diurnal cycle results from the precipitation feature analysis. A proxy for convective fraction (ratio of 40 dBZ to 10 dBZ; Fig. 1a) suggests that convective fraction is highest in the late afternoon (~1700 LT), in accordance with diurnal heating over the SMO. The amplitude on this peak is very large compared to the rest of the cycle. The mean feature maximum dimension (Fig. 1b) shows somewhat different behavior, with the maximum coming later, at 1900 LT, and a small plateau in the early to mid-morning hours.

The importance of large features or mesoscale convective systems (MCSs);

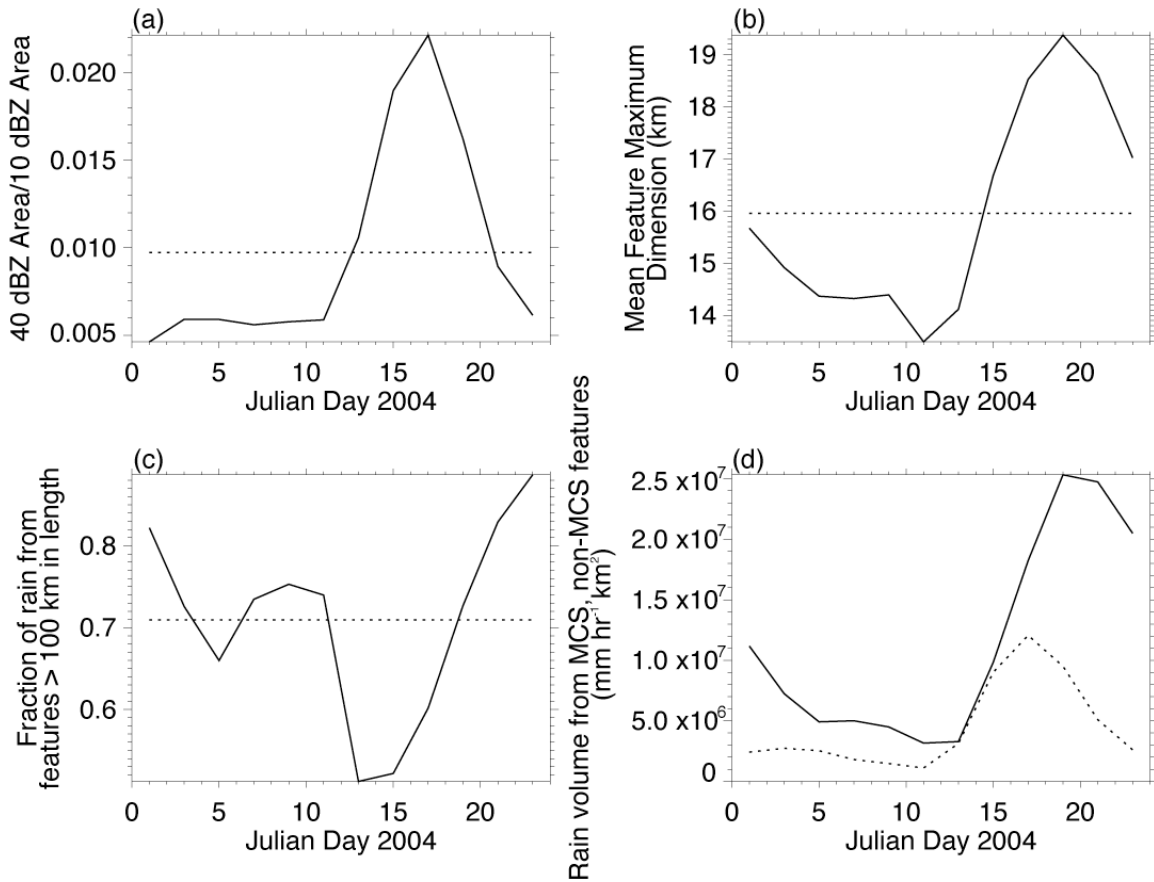


Figure 1. Diurnal cycle of NAME precipitation feature statistics. (a) Ratio of 40 dBZ echo to 10 dBZ echo area. Dotted line is mean value over entire day. (b) Mean feature maximum dimension. (c) Fraction of rain from features greater than 100 km in maximum dimension (defined as MCSs). (d) Rain volume from MCS (solid) and non-MCS (dotted) features.

defined as features > 100 km in maximum dimension) can be seen in the latter half of Fig. 1. The fraction of rainfall from MCSs (Fig. 1c) shows a peak even later in time, near 2300 LT. In addition, there is a secondary maximum in the early to mid-morning hours. This corresponds to coastal MCSs often observed to form along the land breeze during this time period. Total rain volume from MCS and non-MCS features (Fig. 1d) further demonstrates the relative importance of MCSs to rainfall in this region. In addition, note the non-MCS peak that precedes the MCS peak.

Overall, the diurnal cycle results suggest that MCSs are the dominant mode of convection in this region, with respect to rainfall production. The systems grow upscale from smaller convection that develops in the afternoon over the SMO, and forms MCSs during the evening hours. In addition, there is a secondary MCS peak in the morning hours, where systems

develop along the land breeze near the coast.

3. IMPACT OF LARGE-SCALE FORCING

Figure 2 (dates/times UTC, not LT like Fig. 1) shows time series of the ratio of 40 dBZ to 10 dBZ echo (upper left), mean feature maximum dimension (upper right), fraction of rain from MCS features (length > 100 km), and 700 mb u and v winds from the Mazatlan sounding during the NAME extended observing period (EOP). A one-day running mean filter has been applied to the radar data to smooth the time series. The red shading indicates the approximate time periods that Ahijevych et al. (2005) designated as “disturbed”.

There is good rough correspondence between the behavior of precipitation features and the occurrence of disturbed periods. During disturbed periods

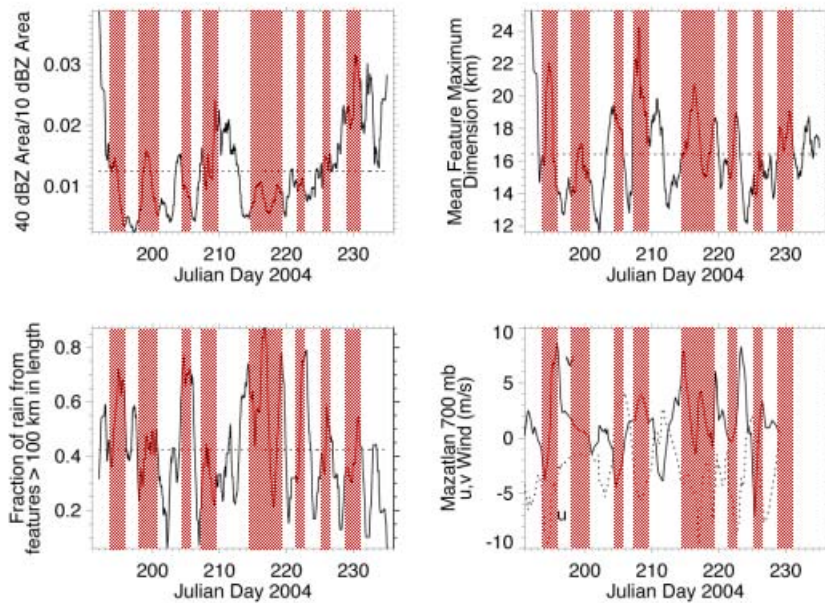


Figure 2. Time series of NAME precipitation feature statistics and Mazatlan 700 mb winds. (a) Ratio of 40 dBZ echo to 10 dBZ echo area. Dotted line is mean value over entire dataset. Shaded red regions are “disturbed” periods. (b) Mean feature maximum dimension. (c) Fraction of rain from features greater than 100 km in maximum dimension (defined as MCSs). (d) Mazatlan sounding 700 mb winds (u – dashed; v – solid).

there tend to be greater convective fraction (based on the 40 dBZ ratio proxy), larger features, and more rain from MCSs.

The presence of fluctuating meridional winds on a 3-5 day time scale in the sounding data suggests the passing of easterly waves, although the first set of strong southerlies early in the EOP (Julian Days 195-196) are due to a Gulf surge caused by Tropical Storm Blas (Higgins et al. 2005). There was a second Gulf surge during days 202-203, which also shows up as weaker southerly flow.

The following discussion points out the generalized behavior of convection relative to the 700 mb winds (i.e., easterly waves). It is important to note beforehand, however, that there are exceptions to this generalized behavior, and that the impact of large-scale forcing is likely more complex. But, to first order, larger features and MCSs tend to occur during the more northerly

phase of the easterly waves, or just on the tail end of this phase. Higher convective fraction leads this behavior, but on a sub-day time scale consistent with the diurnal cycle behavior seen in Fig. 1.

This relationship to easterly wave phase (larger and more organized convection during the northerly phase) is qualitatively similar to that seen in the EPIC project (Petersen et al. 2003). However, the overall convective behavior is complex and may also depend on other factors, such as Gulf surges, easterly wave passage relative to the diurnal cycle, topographic flows, the influence of mid-latitude air masses, and other large-scale events.

Note that during the first Gulf surge (days 195-196), convective behavior is more in sync with the southerly flow, consistent with the influx of moisture associated with these surges. The second Gulf surge shows a weaker relationship with the convection,

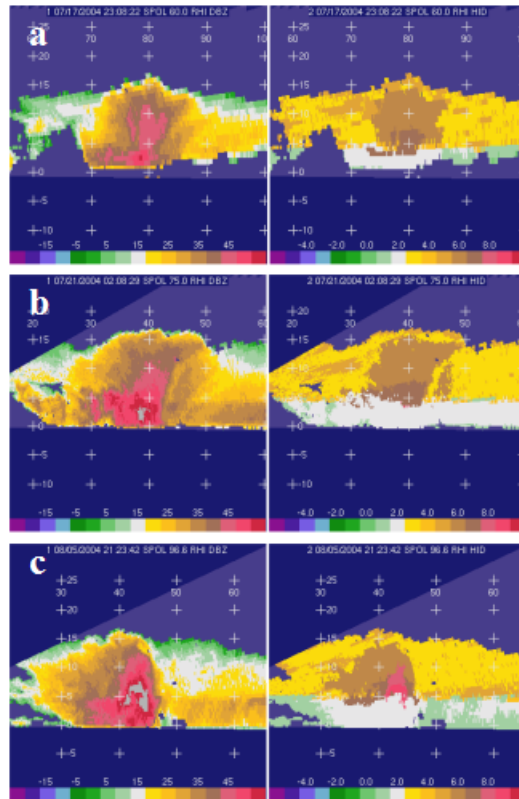


Figure 3. RHIs of reflectivity (left) and hydrometeor classification (right) from S-Pol on three different dates. Dates, UTC times, and azimuth of RHI in degrees are specified in each sub-figure. Hydrometeor classification categories are as follows – unclassified (0; green), drizzle (1; light green), rain (2; white), dry snow (3; yellow), wet snow (4; orange), vertical ice (5; dark orange), low-density graupel (6; brown), high-density graupel (7; dark brown); small hail ($D < 2$ cm; 8; dull red); large hail ($D > 2$ cm; 9; red).

with the latter peaking after the strongest southerlies have occurred. In addition, the Mazatlan winds are not a full proxy for easterly waves and other large-scale weather events. Further large-scale analysis will require use of the full multi-site sounding dataset available for NAME (Higgins et al. 2005).

4. MICROPHYSICAL CASE STUDIES

Work is ongoing for multiple case studies of the microphysical evolution of individual storms, utilizing 3-D data from the S-Pol polarimetric radar. Figure 3 shows sample RHIs from three of these cases. Shown are reflectivity and hydrometeor classification, which was based on the methodology of Tessendorf et al. (2005). The first case, 17 July 2004 (Fig. 3a), is from a disturbed period. It was an intense

multicellular storm over the SMO, with graupel reaching up to nearly 15 km in height (AGL).

The second case, 21 July (Fig. 3b), was an MCS that occurred over the SMO during an undisturbed period. Here we see graupel over 15 km AGL. (Actually, since S-Pol was deployed on the coastal plain near the Gulf, AGL and MSL are roughly equal.) It is important to note, as this figure shows, that disturbed periods did not necessarily contain all the intense convection or MCSs. The disturbed criteria mainly involve long-lived widespread convection or MCSs moving out to sea (Ahijevych et al. 2005). Thus, the criteria are more propagation- and lifetime-oriented, not necessarily dependent on the convective intensity.

The third case, 5 August (Fig. 3c), was an intense MCS that developed over the SMO during a disturbed period. This storm was more intense than the previous

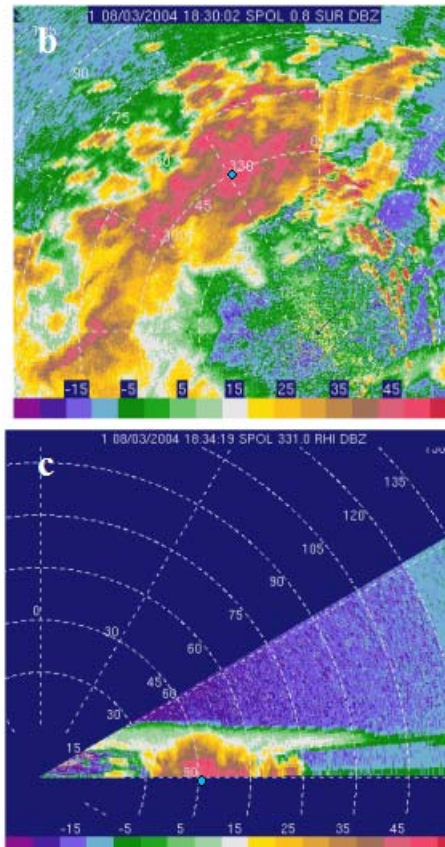
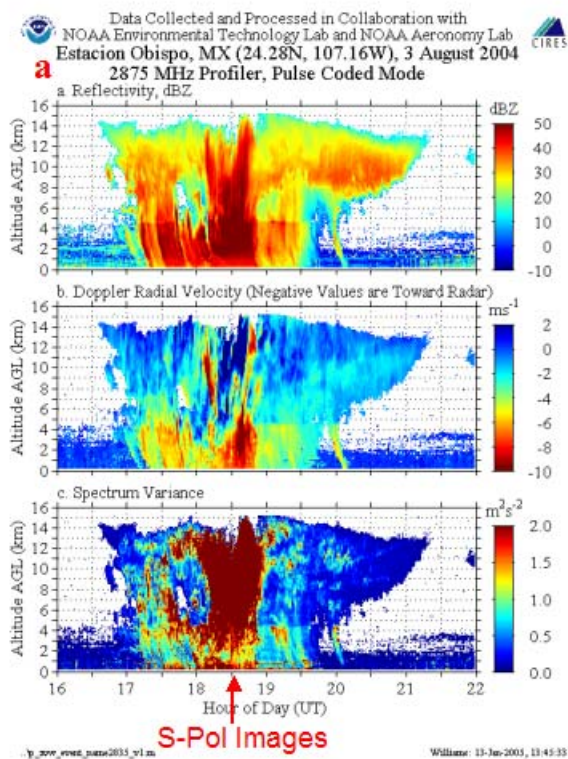


Figure 4. (a) Reflectivity (top), Doppler velocity (middle), and spectral width (bottom) as a function of time and height from the S-band profiler at the NOAA supersite. (b) Low-level PPI of reflectivity from S-Pol at the time noted by the red arrow in (a). The blue dot is the approximate location of the profiler. (c) S-Pol reflectivity RHI over the profiler. Date, UTC time, and sweep angle are listed in each S-Pol plot.

two, as large hail formed aloft, and the storm showed a bounded weak echo region (BWER) with a high-reflectivity (> 60 dBZ) overhang, though the hail melted before reaching the ground.

Overall, there were not a lot of well-organized convective systems during NAME 2004. Though MCSs often occurred, they tended to have a very messy structure, with few examples of the classic leading-line/trailing-stratiform MCSs seen elsewhere. However, as these case studies demonstrate, convective intensity was quite high in this region.

We are currently studying the full evolution of these different cases, as well as the mechanisms responsible for the common occurrence of intense yet poorly organized convective systems. We also are examining the importance of large-scale forcing for microphysical structure and evolution, as well as the relative differences between systems that develop over land and

those that developed in a more oceanic environment.

5. S-POL/PROFILER INTERCOMPARISON

We also are currently doing intercomparisons between the S-Pol radar and the profiler network at the NOAA supersite, which was placed on the coastal plain about 45 km NW of S-Pol. Figure 4 shows a sample case study, 3 August, which was an MCS that occurred during a disturbed period. The S-band profiler data (Fig. 4a) demonstrate the excellent vertical resolution provided by the instrument, showing the small-scale turbulent updrafts and downdrafts. Meanwhile, the S-Pol data (Fig. 4b-c) can be used to provide larger-scale horizontal and vertical context to the profiler data.

Some of the ongoing profiler/S-Pol intercomparison work is modeled after May

and Keenan (2005), comparing S-Pol drop size distribution and hydrometeor classification retrievals to those provided by the profiler network. In addition, we will use the profiler network to retrieve updraft information, providing valuable kinematic data for comparison with the observed microphysical evolution of these storms.

6. DISCUSSION AND CONCLUSIONS

This paper shows some of the ongoing NAME radar work occurring at Colorado State University. Though our work is at early stages, the dataset shows great promise in providing better understanding of precipitation in this region, including the effects of the diurnal cycle and large-scale forcing; kinematic, microphysical, and mesoscale structure and evolution of individual systems; and other importance science questions pertinent to the North American monsoon.

7. ACKNOWLEDGMENTS

We thank Jon Lutz and Bob Rilling of NCAR, Arturo Valdez-Manzanillo of the University of Tabasco, and Armando Rodriguez of SMN, as well as other NCAR S-Pol and SMN radar staff, for their help with data collection and quality control. This work was funded by NSF grant ATM-0340544 and NOAA grant NA17RJ1228.

8. REFERENCES

Ahijevych, D. A., R. E. Carbone, T. J. Lang, and A. V. Manzanillo, 2005: The diurnal cycle of rainfall and the identification of rainfall regimes within the North American monsoon of NW Mexico. *32nd Conf. on Radar Meteorol.*, Amer. Meteorol. Soc., Albuquerque, NM.

Higgins, W., et al., 2005: The North American Monsoon Experiment (NAME) 2004 field campaign and modeling strategy. Submitted to *Bull. Amer. Meteorol. Soc.*

Lang, T. J., R. Cifelli, L. Nelson, S. W. Nesbitt, G. Pereira, S. A. Rutledge, D. Ahijevych, and R. Carbone, 2005: Radar observations during NAME 2004. Part I: Data products and quality control. *32nd Conf. on Radar Meteorol.*, Amer. Meteorol. Soc., Albuquerque, NM.

May, P. T., and T. D. Keenan, 2005. Evaluation of microphysical retrievals from polarimetric radar with wind profiler data. *J. Appl. Meteorol.*, **44**, 827-838.

Nesbitt, S. W., E. J. Zipser, and D. J. Cecil, 2000: A census of precipitation features in the Tropics using TRMM: Radar, ice scattering, and lightning observations. *J. Climate*, **13**, 4087-4106.

Nesbitt, S. W., R. Cifelli, and S. A. Rutledge, 2005: Storm morphology and rainfall characteristics of TRMM precipitation features. Submitted to *Mon. Wea. Rev.*

Petersen, W. A., R. Cifelli, D. J. Boccippio, S. A. Rutledge, and C. Fairall, 2003: Convection and easterly wave structures observed in the eastern Pacific warm pool during EPIC-2001. *J. Atmos. Sci.*, **60**, 1754-1773.

Tessendorf, S. A., L. J. Miller, K. C. Wiens, and S. A. Rutledge, 2005: The 29 June 2000 supercell observed during STEPS. Part I: Kinematics and microphysics. Accepted in *J. Atmos. Sci.*